Control Mechanism for Alumina Dissolution in Cryolite Melts

Ž. LUBYOVÁ and V. DANĚK

Institute of Inorganic Chemistry, Slovak Academy of Sciences, SK-842 36 Bratislava

Received 1 March 1994

The process determining the alumina dissolution rate in cryolite-based melts containing increased amount of AlF_3 and CaF_2, KF and LiF as additives, was studied. The influence of KF on the equilibrium solubility of Al_2O_3 in these melts was investigated.

It was found that the dissolution rate of alumina in the cryolite-based melts may be limited by diffusion or heat transfer. Which of these processes becomes the control one is determined by the specific surface and the starting mass of Al_2O_3, its solubility in the given melt, and the convection of electrolyte.

The effort to substitute the conventional electrolyte, commonly used in the aluminium industry, by electrolytes with lower temperature of primary crystallization evokes the need to study the solubility and the dissolution kinetics of Al_2O_3 in these electrolytes. Innovative electrolytes are cryolite-based melts with increased content of AlF_3 (> 14 mass %) and LiF, KF, and CaF_2 (or MgF_2) as additives [1—3].

A number of papers devoted to the study of alumina dissolution in the conventional electrolytes may be found in the literature. However, the view on the dissolution mechanism and the most probable process determining the dissolution rate differs. One group of authors supposes that the dissolution is controlled by diffusion and their works involve the measurement of diffusion coefficients [4—10]. On the other hand, the authors of [11, 12] suppose, on the basis of the determined higher values of the activation energy of the diffusion, that dissolution-precipitation is the control process. Moreover, based on the observation that the alumina dissolution in cryolite melts is the endothermic process with an uncommon heat effect the authors of [13—15] suppose the heat transfer to be the most probable control process.

In the present work the solubility and the dissolution mechanism of industrial polydisperse aluminium oxides in cryolite melts with higher content of AlF_3 and with CaF_2, KF, and LiF as additives were studied. The dissolution kinetics under stationary conditions, *e.g.* without forced convection, at constant temperature and with starting alumina mass equal to the amount needed for the saturation was investigated. It was supposed that at the given experimental conditions the limiting dissolution process may be either diffusion or heat transfer and that free convection due to the density gradient takes place during the dissolution of alumina. The kinetic model proposed for dissolution of dispersed particles controlled by convective diffusion [16, 17] and the model proposed for the dissolution controlled by heat transfer into the reaction area [18—20] were verified.

For the dissolution of dispersed particles controlled by the convective diffusion, if the dissolution involves the change in the contact surface and the starting alumina amount, m_0, equals the amount needed for saturation, m_s, it holds [16, 17]

$$m^{-2/3} - m_0^{-2/3} = k \cdot t \qquad (1)$$

where m is the mass of solid in time t.

For the dissolution of dispersed particles controlled by heat transfer the following relation was derived [18, 19]

$$m_0^{1/3} - m^{1/3} = k' \cdot t \qquad (2)$$

The rate constant k involves the diffusion coefficient, while the rate constant k' involves the heat transfer coefficient. The detailed analysis of these processes can be found in [16—19]. Relations (*1*) and (*2*) were derived for monodispersed spherical solid particles. However, they are valid also for nonisometric particles, when their shape remains approximately constant during dissolution, as well as for narrow fractions of polydispersed systems [17]. In our previous works [21, 22] we found that during dissolution in cryolite melts the shape of alumina grains does not substantially change and that the most alumina powders industrially used show narrow particle distribution. The next important fact, which enables to apply the above relations, is the slowed sinking of the very porous alumina [21, 22]. The theoretical density of porousless alumina is 3.97 g cm^{-3}, while that of the industrial aluminas, determined by means of mercury porosimetry, is in the range of 1.9—2.5 g cm^{-3} [21, 22].

EXPERIMENTAL

Cryolite, Na_3AlF_6, was synthesized from NaF ("for monocrystals", Turnov) and AlF_3, sublimated from technical product (Slovak Technical University, Bratislava). CaF_2 ("for monocrystals", Turnov), KF (anal. grade, Lachema, Brno), and LiF ("for monocrystals", Turnov) were used as additives.

The values of the equilibrium solubility of alumina in the investigated melts were determined using the method of the isothermal saturation [23] or they were calculated according to the empirical equation published in [24]. The amount of alumina dissolved in the melt was determined using the gravimetric method dissolving the finely ground samples in boiling $AlCl_3$ solution and calcinating the undissolved remainder (Al_2O_3) [23]. The experimental error in the determination of the dissolved alumina content was approximately ± 0.5 mass %.

Two alumina of different provenience were used for the dissolution kinetics investigation:

Al_2O_3 from ZSNP, Žiar nad Hronom, Slovakia,

Al_2O_3 from Comalco, Australia.

The dissolution rate was measured in different melt compositions at three different temperatures:

880 °C in the melts of the composition:

1. (74 mass % Na_3AlF_6 + 26 mass % AlF_3) + + 3 mass % CaF_2

2. (74 mass % Na_3AlF_6 + 26 mass % AlF_3) + + 3 mass % CaF_2 + 3 mass % KF

3. (74 mass % Na_3AlF_6 + 26 mass % AlF_3) + + 3 mass % CaF_2 + 3 mass % LiF

980 °C in the melts of the composition:

4. (78 mass % Na_3AlF_6 + 22 mass % AlF_3) + + 3 mass % CaF_2

5. (78 mass % Na_3AlF_6 + 22 mass % AlF_3) + + 3 mass % CaF_2 + 3 mass % KF

950 °C in the melts of the composition *5.*

Approximately 40 g of the investigated electrolyte was weighted into the platinum crucible and melted in an electric resistance furnace for the desired temperature. Aluminium oxide in the amount needed for the saturation of the electrolyte at the given temperature was then added using the silica tube. Samples of the melt were then taken away in the time intervals of 10, 30, 60, 90, and 120 min in which the content of dissolved alumina was determined by the gravimetric method [23].

For the characterization of the aluminium oxides used the X-ray phase analysis and the scanning electron microscope Jeol X 5C were used. The specific surface of the alumina powders was determined by the BET method using the Sorptomatic 1800 device and the specific surface of pores was determined using the C. Erba mercury porosimeter.

RESULTS AND DISCUSSION

The solubility of alumina in different cryolite-based melts is given in Table 1. From the values it follows that the solubility of alumina in the melt of the composition (74 mass % Na_3AlF_6 + 26 mass % AlF_3) + 3 mass % CaF_2 at 880 °C is lower than the solubility in the melt of the composition (78 mass % Na_3AlF_6 + 22 mass % AlF_3) + 3 mass % CaF_2 at the temperature of 980 °C. The addition of 3 mass % KF, resp. LiF to the melt at 880 °C causes only little change of the solubility, while the addition of 3 mass % KF at 980 °C evidently increases the alumina solubility. The change of temperature by 30 °C does not substantially affect the alumina solubility.

Table 1. Maximum Solubility of Aluminium Oxide in Cryolite-Based Melts

Melt composition w/%	θ/°C	w_s/%
(74 Na_3AlF_6 + 26 AlF_3) + 3 CaF_2	880	5.04*
(74 Na_3AlF_6 + 26 AlF_3) + 3 CaF_2 + 3 KF	880	5.31
(74 Na_3AlF_6 + 26 AlF_3) + 3 CaF_2 + 3 LiF	880	4.60*
(78 Na_3AlF_6 + 22 AlF_3) + 3 CaF_2	980	7.74*
(78 Na_3AlF_6 + 22 AlF_3) + 3 CaF_2 + 3 KF	980	9.40
(78 Na_3AlF_6 + 22 AlF_3) + 3 CaF_2 + 3 KF	950	8.80

* Calculated according to Ref. [24].

The dissolution kinetics was followed with two different types of alumina. The microphotographs of the grains of both industrial alumina powders are shown in Fig. 1*a* and *b*. In [21, 25] it was found that the industrial alumina powders show high specific surface and high porosity of the grains. These properties affect the amount of the dissolved Al_2O_3 especially in the first stage of the dissolution process [21]. Therefore, the values of the average grain diameter, d_{mean}, determined by direct measurement from the microphotographs, the specific powder surface, determined using the BET method, S_{BET}, and the specific surface of pores, S_{por}, determined using the mercury porosimeter, are given in Table 2 for illustration.

The dependence of the dissolved alumina amount on the dissolution time for the investigated melts, aluminium oxides, and temperature used is given in Tables 3 and 4. The amount of the undissolved Al_2O_3, m, in time t was calculated from the starting amount of the added alumina, m_s, and the determined amount of alumina dissolved in the melt, w, in time t. From Table

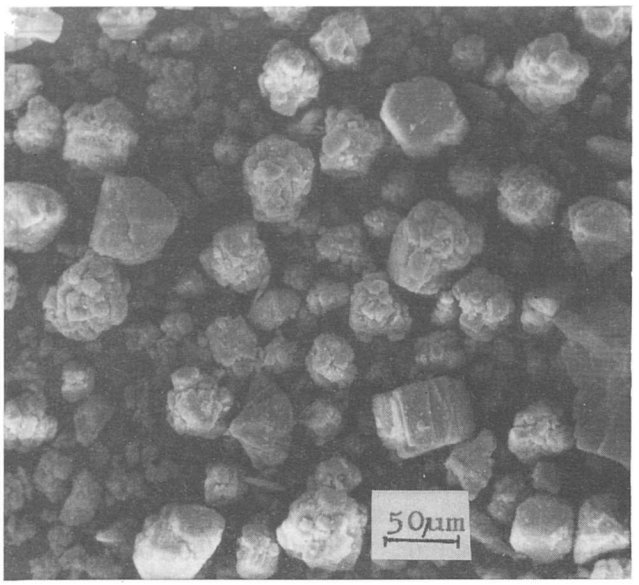

a

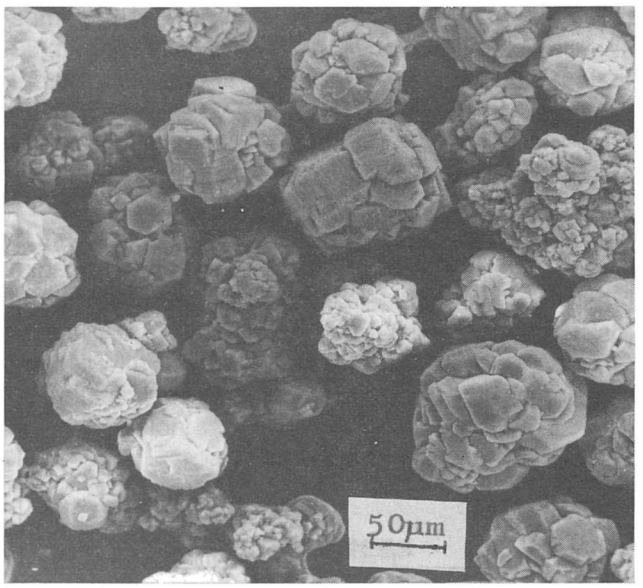

b

Fig. 1. *a*) Microphotograph of the Al_2O_3 grains from ZSNP, Žiar nad Hronom, Slovakia; *b*) microphotograph of the Al_2O_3 grains from Comalco, Australia.

3 it is obvious that for the first series of measurements at 880 °C the determined content of the dissolved alumina for all the melts (*1*—*4*) is approximately the same within the experimental error. The addition of 3 mass % KF, resp. LiF, like in the case of the alumina solubility, does not affect the alumina dissolution rate. Also in the second series of measurements, at the temperature of 980 °C (*cf.* Table 4), the KF addition does not affect the alumina dissolution rate in spite of its evident influence on the alumina solubility. Higher content of

Table 2. Values of the Average Grain Diameter, d_{mean}, Specific Surface, S_{BET}, and Specific Pore Surface, S_{por}, for the Investigated Alumina Powders

Al_2O_3	$d_{mean}/\mu m$	$S_{BET}/(m^2\,g^{-1})$	$S_{por}/(m^2\,g^{-1})$
Žiar nad Hronom	19.7	58.1	35.2
Comalco	79.7	64.0	13.1

Table 3. Experimentally Determined Amounts of Dissolved Al_2O_3 after the Dissolution Time *t* for the Investigated Melts at 880 °C

No.	Al_2O_3	Melt composition *w*/%	*t*/min	*w*/%	*m*/g
1	Comalco	(74 Na_3AlF_6 + 26 AlF_3) + 3 CaF_2	10	2.9, 2.5, 3.3	0.90, 1.07, 0.73
			30	3.6, 3.2	0.60, 0.77
			60	4.7, 3.7, 4.0	0.14, 0.56, 0.44
			90	4.4, 4.2	0.27, 0.35
			120	4.3, 4.5, 4.7	0.31, 0.23, 0.14
2	Comalco	(74 Na_3AlF_6 + 26 AlF_3) + 3 CaF_2 + 3 KF	13	2.4, 3.2	1.21, 0.88
			30	3.0, 3.4	0.96, 0.88
			61	4.0, 4.0	0.55, 0.55
			92	4.1, 4.5	0.50, 0.34
			123	4.3, 4.7	0.42, 0.25
3	Žiar nad Hronom	(74 Na_3AlF_6 + 26 AlF_3) + 3 CaF_2 + 3 KF	11	2.7	1.10
			30	3.2	0.89
			60	4.2	0.47
			90	4.3	0.43
			120	5.1	0.09
4	Žiar nad Hronom	(74 Na_3AlF_6 + 26 AlF_3) + 3 CaF_2 + 3 LiF	12	2.6	0.84
			29	3.2	0.59
			60	3.4	0.50
			89	3.7	0.38
			120	4.0	0.25

Table 4. Experimentally Determined Amounts of Dissolved Al_2O_3 after the Dissolution Time *t* for the Investigated Melts at 950 °C (*7*) and 980 °C (*5*, *6*)

No.	Al_2O_3	Melt composition *w*/%	*t*/min	*w*/%	*m*/g
5	Žiar nad Hronom	(78 Na_3AlF_6 + 22 AlF_3) + 3 CaF_2	10	4.6	1.29
			30	7.0	0.37
			90	7.1	0.35
			120	7.8	0.07
6	Žiar nad Hronom	(78 Na_3AlF_6 + 22 AlF_3) + 3 CaF_2 + 3 KF	11	5.6	1.48
			30	6.6	1.07
			62	7.8	0.57
			89	8.5	0.79
7	Žiar nad Hronom	(78 Na_3AlF_6 + 22 AlF_3) + 3 CaF_2 + 3 KF	11	5.4	1.33
			35	6.5	0.84
			66	7.3	0.49
			91	7.9	0.22

dissolved alumina was determined only in the first analyzed sample after 10 min of dissolution.

The most probable mechanism of the alumina dissolution in the cryolite-based melts was determined using the statistical regression analysis looking for the linear fit for eqns (*1*) and (*2*), respectively. Since the obtained experimental results for the melts *1*—*4* and *5*—*7* may be regarded within the experimental error as similar, two data sets, *1*—*4* and *5*—*7*, respectively, were created for the statistical regression analysis.

The regression analysis of the *1*—*4* data set showed (Table 5) that for the description of the dissolution of alumina in the acidic melt at 880 °C the linear fit was obtained for the equation

$$m^{-2/3} - m_0^{-2/3} = k_0 + k_1 \cdot t \qquad (3)$$

The linear time dependence of the dissolved alumina amount (Fig. 2) confirms that the dissolution of alumina in the acidic melts at 880 °C is controlled by diffusion. The polynomial regression of eqn (*2*) yields the fourth-order equation which does not comply with the theory.

Table 5. Coefficients k_0, k_1, and k_2 of Regression Equations, and the Standard Deviations of Approximation, s, for the Process Controlled by Diffusion (Eqn (*1*)) and by Heat Transfer (Eqn (*2*))

θ/°C	Control process	
	Diffusion	Heat transfer
	$m^{-2/3} - m_0^{-2/3} = k_0 + k_1 \cdot t + k_2 \cdot t^2$	$m_0^{1/3} - m^{1/3} = k_0 + k_1 \cdot t^2 + k_2 \cdot t^4$
880	k_0/g$^{-2/3}$ = 0.26 ± 0.04	k_0/g$^{1/3}$ = 0.30 ± 0.01
	k_1/(g$^{-2/3}$ s^{-1}) = (1.09 ± 0.09)×10^{-2}	k_1/(g$^{1/3}$ s^{-2}) = (5.49 ± 0.71)×10^{-5}
	s = 0.13	k_2/(g$^{1/3}$ s^{-4}) = (−2.31 ± 0.52)×10^{-9}
		s = 0.05
980	k_0/g$^{-2/3}$ = 0.37 ± 0.05	k_0/g$^{1/3}$ = 0.45 ± 0.03
	k_2/(g$^{-2/3}$ s^{-2}) = (1.97 ± 0.29)×10^{-4}	k_1/(g$^{1/3}$ s^{-2}) = (4.94 ± 0.87)×10^{-5}
	s = 0.17	s = 0.10

From the regression analysis of the *5*—*7* data set it follows that for the dissolution of alumina in the cryolite-based melts at 950 °C and 980 °C the following equation holds (Fig. 3)

$$m_0^{1/3} - m^{1/3} = k_0 + k_1 \cdot t^2 \qquad (4)$$

The dissolution of alumina at these temperatures is controlled by heat transfer. The second-order polynomial was obtained for the diffusion-controlled process (eqn (*1*)) which does not comply with the theory.

The coefficients k_0, k_1, and k_2 of the regression equations and the standard deviations of the approximation are given in Table 5. The absolute term k_0 is in both cases statistically important, which indicates that a short preceding process, most probably the surface reaction, takes place before the main control process.

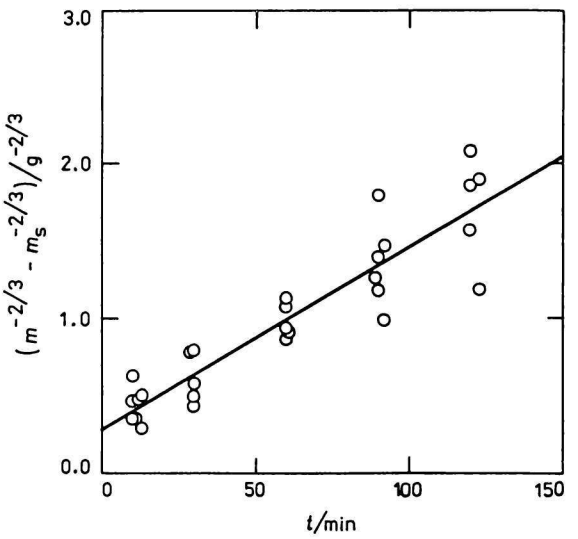

Fig. 2. Regression analysis for dissolution of Al_2O_3 in cryolite melts at 880 °C (*1*—*4* data set).
$m^{-2/3} - m_0^{-2/3} = (0.26 \pm 0.04)\ g^{-2/3} + (1.09 \pm 0.09) \times 10^{-2}\ g^{-2/3}\ s^{-1}\ t$

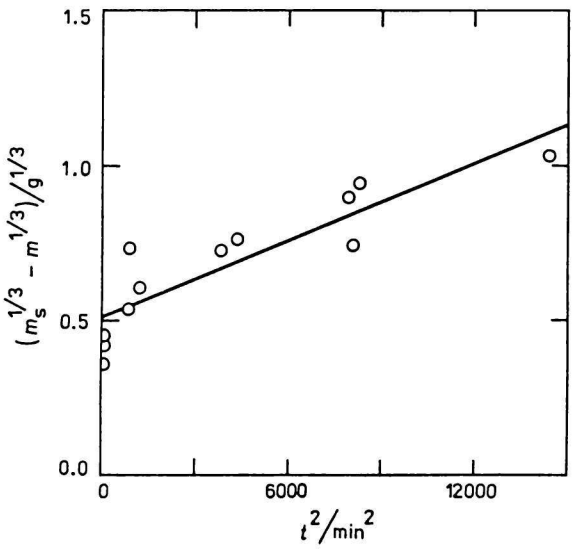

Fig. 3. Regression analysis for dissolution of Al_2O_3 in cryolite melts at 950 °C and 980 °C (*5*—*7* data set).
$m_0^{1/3} - m^{1/3} = (0.45 \pm 0.03)\ g^{1/3} + (4.94 \pm 0.87) \times 10^{-5}\ g^{1/3}\ s^{-2}\ t^2$

From the results of this work it follows that the alumina dissolution rate in cryolite melts may be limited by diffusion or by heat transfer. Which from these processes becomes the limiting one will be determined by the initial stage of dissolution. In [15, 26] it was found that the most expressive temperature drop is caused by the first part of dissolved alumina. The more alumina dissolves in the initial stage, the bigger is the temperature drop. If the temperature drop in the initial stage is expressive enough, the heat transfer becomes the limiting process, because the temperature may de-

crease below the temperature of primary crystallization and a new phase crystallizes on the alumina grain surface. Further dissolution of alumina is then possible only after its melting, which is conditioned by the heat transfer.

From [15, 26] it follows that the temperature drop of the melt in the initial stage of dissolution depends on the specific surface, the solubility and the amount of added alumina, and on stirring. The experimental conditions in the present work were in both series equal. Only the solubility of alumina was changed from approx. 5 mass % at 880 °C to approx. 9 mass % at 950 °C and 980 °C. It may be supposed that in the *1—4* data set due to the lower solubility and consequently the lower driving force the amount of dissolved alumina in the first stage is lower than in the *5—7* data set. The temperature drop in the *1—4* data set is not sufficient for the heat transfer to become the limiting process.

Using the X-ray phase analysis it was found that both aluminium oxides used have approximately the same phase composition, *i.e.* 70 mass % α-Al_2O_3 and 30 mass % γ-Al_2O_3. However, no correlation between the dissolution rate and the phase composition of industrial aluminium oxides has been found, regardless even of their specific surface area [27].

On the basis of the obtained results it may be also assumed that with regard to the high specific surface of the industrial aluminium oxides the dissolution of alumina in the conventional electrolytes with higher working temperature and higher alumina solubility will be controlled by heat transfer. In the low-temperature electrolytes with lower working temperature and low alumina solubility the dissolution of alumina will be controlled by diffusion.

REFERENCES

1. Thonstad, J. and Solheim, A., *Aluminium 62*, 938 (1986).
2. Grjotheim, K., Kvande, H., and Welch, B. J., *Light Metals 1986,* 417.
3. Sterten, A., Skybakmoen, S., Solheim, A., and Thonstad, J., *Light Metals 1988,* 663.
4. Shurygin, P. M., Boronenkov, V. N., and Kryuk, V. Yu., *Izv. Vyssh. Ucheb. Zaved., Tsvetn. Metall. 5*, 52 (1962).
5. Shurygin, P. M., Barunin, L. N., and Boronenkov, V. N., *Izv. Vyssh. Ucheb. Zaved., Tsvetn. Metall. 5*, 106 (1962).
6. Shurygin, P. M., Boronenkov, V. N., and Kryuk, V. Yu., *Sobr. Nauch. Tr. Uralsk. Politekh. Inst.* No. 126, 80 (1963).
7. Desclaux, P. and Rolin, M., *Rev. Inst. Hautes Temp. Refract. 8*, 227 (1971).
8. Thonstad, J., *Electrochim. Acta 14*, 127 (1969).
9. Gerlach, J., Henning, U., and Plotsch, H. D., *Erzmetall 31*, 339 (1978).
10. Gerlach, J., Henning, U., and Plotsch, H. D., *Erzmetall 31*, 496 (1978).
11. Kachanovskaya, I. S., Osovik, V. Yu., and Kukhotkina, T. N., *Tsvet. Met. 44*, 40 (1972).
12. Thonstad, J., Nordmo, F., and Paulsen, J. B., *Metall. Trans., A3*, 403 (1972).
13. Bertaud, Y. and Lectard, A., *J. Metals 11*, 22 (1984).
14. Taylor, M. P., Liu, X., Frazer, K. J., and Welch, B. J., *Light Metals 1990,* 259.
15. Liu, X., Purdie, J. M., Taylor, M. P., and Welch, B. J., *Light Metals 1991,* 289.
16. Hixson, A. W. and Crowell, J. H., *Ind. Eng. Chem. 32*, 923 (1931).
17. Hlaváč, J., *Silikáty 7*, 242 (1963).
18. Sattergield, C. N. and Feakes, F., *AIChE J. 5*, 115 (1959).
19. Narsimham, G., *Chem. Eng. Sci. 16*, 7 (1961).
20. Šesták, J., *Měření termofyzikálních vlastností pevných látek.* (Measurement of Thermophysical Properties of Solids.) Academia, Prague, 1982.
21. Lubyová, Ž., Gabčová, J., and Khandl, V., *Hutn. Listy 48*, 31 (1993).
22. Lubyová, Ž. and Daněk, V., *Aluminium 71,* 346 (1995).
23. Lubyová, Ž., Fellner, P., and Gabčová, J., *Chem. Papers 47*, 218 (1993).
24. Skybakmoen, E., Solheim, A., and Sterten, A., *Light Metals 1990,* 317.
25. Garcia Coque, P., Llavona, M. A., Ayala, M. J., and Sancho, J. P., *Light Metals 1991,* 193.
26. Matiašovský, K. *et al., Res. Report, Inst. Inorg. Chem., Slovak Acad. Sci.,* Bratislava, 1987.
27. Bagshaw, A. N. and Welch, B. J., *Light Metals 1986,* 35.

Translated by V. Daněk